Resolvent operator approach to manybody perturbation theory. II. Open shells

Ajit Banerjee, Debashis Mukherjee, and Jack Simons

Articles you may be interested in

Restricted openshell Hartree–Fockbased manybody perturbation theory: Theory and application of energy and gradient calculations
J. Chem. Phys. **97**, 6606 (1992); 10.1063/1.463664

Erratum: Resolvent operators approach to manybody perturbation theory. III. Applications [J. Chem. Phys. 7 6, 1995 (1982)]
J. Chem. Phys. **77**, 2219 (1982); 10.1063/1.444456

Resolvent operator approach to manybody perturbation theory. III. Applications
J. Chem. Phys. **76**, 1995 (1982); 10.1063/1.443172

Resolvent operator approach to manybody perturbation theory. I. Closed shells
J. Chem. Phys. **76**, 1972 (1982); 10.1063/1.443170

Manybody perturbation theory applied to electron pair correlation energies. II. Closedshell secondrow diatomic hydrides
J. Chem. Phys. **64**, 4578 (1976); 10.1063/1.432091

Resolvent operator approach to many-body perturbation theory. II. Open shells

Ajit Banerjee, Debashis Mukherjee,[a] and Jack Simons[b]

Department of Chemistry, University of Utah, Salt Lake City, Utah 84112
(Received 7 July 1981; accepted 12 October 1981)

In this paper, we develop a time-dependent approach to many-body perturbation theory for open shells based on the resolvent of the Schrödinger equation. We introduce, analogous to the closed-shell case, quantities $S_{ij}(t) = i <\phi_i|e^{-i(H-E_c)t}|\psi_j>/<\psi_j^0|\psi_j>$, where ψ_j^0 and ψ_j are the jth unperturbed and exact functions, respectively. The ψ_j^0's can be expressed in terms of "model space" functions $\phi_i = \Omega_i^+|\phi>$, where the Ω_i^+ are appropriate creation/annihilation operator products acting on a conveniently chosen closed-shell vacuum ϕ. These ϕ_i's are not necessarily degenerate with respect to the unperturbed Hamiltonian H_0. E_c is the exact (correlated) energy of the vacuum ϕ. The Fourier transforms $S_{ij}(\omega)$ of $S_{ij}(t)$ have the form $S_{ij}(\omega) = <\phi_i|(\omega + E_c - H)^{-1}|\psi_j>/<\psi_j^0|\psi_j>$ and thus have poles at energy differences $(E_j - E_c)$, i.e., relative to the *exact* vacuum energy. Using the time-dependent perturbation expansion of $S(t)$, we obtain a Dyson-like equation $\bar{N}^{-1}(\omega) = \bar{N}^{0-1}(\omega) + \Sigma$, where $\bar{N}$ is defined as $\bar{N}_{ij}(\omega) = <\phi_i|(\omega + E_c - H)^{-1}|\phi_j>$ and $\bar{N}^0$ is the corresponding unperturbed component. Knowledge of the combining coefficients C_{ji} in $\psi_j^0 = \Sigma_i C_{ji}\phi_i$ is thus not required for finding the poles. We arrive at the Dyson-like equation by first eliminating closed diagrams and then regrouping the remaining terms in the perturbation series for S into "top" and "bottom" parts. Regrouping appropriate to the Brillouin–Wigner (BW) case together with an associated time-integration procedure yields Σ^{BW} which consists of disconnected and ω-dependent diagrams. This is shown to yield the open-shell BW series in the Bloch–Horowitz form. An alternative regrouping procedure and use of the "folding technique" of Johnson and Baranger leads to a Σ^{RS} which is ω-independent, Hermitian, contains connected diagrams only, and is, thus, size-consistent.

I. INTRODUCTION

In the preceding paper[1] (hereafter called paper I) we developed a time-dependent (TD) many-body perturbation theory (MBPT) from the resolvent of the Schrödinger equation (SE), and we derived both the Brillouin–Wigner (BW) and Rayleigh–Schrödinger (RS) series for the energy of closed-shell systems. In this paper we extend this idea to the open-shell problem.

For open-shell systems, the unperturbed wave function Ψ^0 may contain several determinants. Thus, in contrast to the closed-shell case, the unperturbed wave function cannot be characterized by a *unique* spin–orbital occupancy; therefore, a straightforward application of Wick's theorem[2] is not possible. Furthermore, due to the degeneracy (or near degeneracy) among the determinants of Ψ^0, various alternative choices for the combining coefficients of the determinants may be possible. This has led to the development of several open-shell MBPT's of seemingly different structure.[4–11]

The first step in the development of our open-shell theory is to introduce a vacuum Φ, chosen to be a closed-shell determinant, which may have fewer, greater, or the same number of electrons as the unperturbed function Ψ^0. The vacuum Φ is then related to each of the determinants Φ_i in Ψ^0 through a set of creation, annihilation, or creation/annihilation operator products $\{\Omega_i^+\}$: $|\Phi_i> = \Omega_i^+|\Phi>$. Since, as will be shown later, the energies computed in the MBPT developed here are given relative to the vacuum's energy E_c, the interpretation of the energy shift $\Delta E = E - E_c$ is dictated

by the choice of the vacuum. For example, if Φ contains n fewer particles than Ψ^0, ΔE represents the *correlated* energy shift due to the addition of n electrons. Thus, for the ground state of Be with the model space functions $\{\Phi_i\}$ as $1s^2 2s^2$ and $1s^2 2p^2$, we may choose the vacuum to be the closed-shell Be^{+2} configuration $1s^2$. The calculated MBPT energy shift would then be given relative to the fully correlated Be^{+2} ground state and would correspond to the double electron affinity of Be^{+2}. In contrast, for the closed-shell systems treated in I, where the vacuum is the unperturbed function itself, the calculated energy shift is the correlation energy. We emphasize here that we are able to treat problems where the model space functions $\{\Phi_i\}$ in Ψ^0 are degenerate (e.g., when multideterminant functions are used only to give proper space and spin symmetry) as well as nondegenerate multideterminantal functions (as in the Be case discussed above). We refer to both of these cases as "open-shell" cases.

The subsequent steps in the development of our open-shell MBPT can be outlined as follows. We introduce a matrix $S(\epsilon)$ involving the resolvent of the SE $(\epsilon - H)^{-1}$ and obtain a Dyson-like equation giving the energy shifts ΔE as poles of S. The effective Hamiltonian matrix Σ appearing in the Dyson equation contains up to n-body operators, where n is the number of creation annihilation operators in the Ω_i^*. A partitioning of the terms in the expansion of S similar to that used in the closed-shell BW case leads us to the open-shell BW theory in which Σ is of the Bloch–Horowitz[3] form. An alternative partitioning of the expansion of S similar to that employed in the closed-shell RS case yields a corresponding Σ in RS form. The RS development requires use of the idea of "folding."[4,9] We have chosen to utilize the Johnson–Baranger technique of folding since it has the

[a]Visiting Associate Professor. Permanent address: Theory Group, Department of Physical Chemistry, Indian Association for the Cultivation of Science, Calcutta 700-032, India.
[b]Camille and Henry Dreyfus Fellow, Guggenheim Fellow.

advantage of keeping Σ Hermitian. For the RS case, we give explicit expressions for calculating individual state energies and energy differences for a suitable choice of the vacuum Φ.

II. GENERAL DEVELOPMENTS

We represent the total electronic Hamiltonian of the system as

$$H = H_0 + V , \tag{1}$$

where the unperturbed Hamiltonian H_0 is a conveniently chosen one-particle operator whose exact nature we discuss in Sec. IV. We denote by $\{\Phi_i\}$ a set of determinants which are assumed to be exactly degenerate eigenfunctions of H_0, and we represent the vacuum (which is a closed-shell determinant) as Φ. The assumption of exact degeneracy is made here to keep the development as straightforward as possible. In Sec. IV, we demonstrate how this restriction can be lifted so that we can treat, within the *same* formalism, nondegenerate cases. The orbitals occupied in Φ are called "holes," whereas the unoccupied orbitals are called "particles." All the orbitals are assumed to be eigenfunctions of the one-electron operator h_0 which comprises $H_0 : \sum_i h_0(i) = H_0$. In this hole-particle (h–p) representation, the determinants Φ_i can be written in terms of the vacuum as

$$|\Phi_i\rangle = \Omega_i^+ |\Phi\rangle , \tag{2}$$

where the $\{\Omega_i^+\}$ are products of appropriately chosen hole and/or particle creation operators. We call the space spanned by the set $\{\Phi_i\}$ the model (or reference) space. Notice that the vacuum Φ is also an eigenstate of H_0 with an eigenvalue E_0.

To proceed with our development, we need an analog of the Gellman–Low adiabatic theorem[2] for an open-shell state which adiabatically connects an exact state Ψ_{jH} in the Heisenberg representation at time $t = 0$ to a corresponding unperturbed state Ψ_j^0 of H_0. The state Ψ_j^0 is expressed as a linear combination of the degenerate set $\{\Phi_i\}$:

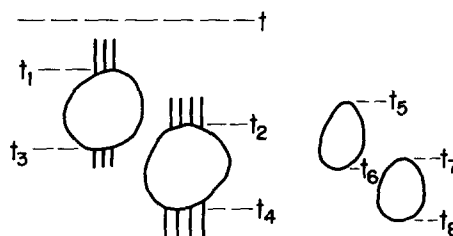$$\Psi_j^0 = \sum_i C_{ij} \Phi_i . \tag{3}$$

FIG. 1. A typical term of the expansion in $N_{ij}(t)$ of Eq. (8). The closed components of the diagram (with time arguments t_5, t_6, t_7, t_8) correspond to the completely contracted operators. The rest of the diagram has uncontracted operators depicted as open lines attached to the blocks with time arguments t_1, t_3, t_2, t_4. As explained in the text, for a nonvanishing contribution to $N_{ij}(t)$ the lines should be valence lines only.

The Gellman–Low adiabatic theorem for open shells[12] can be expressed as

$$\frac{|\Psi_{jH}\rangle}{\langle \Psi_j^0 | \Psi_{jH}\rangle} = \frac{U_I(0, -\infty) |\Psi_j^0\rangle}{\langle \Psi_j^0 | U_I(0, -\infty) |\Psi_j^0\rangle} , \tag{4}$$

where U_I is the evolution operator in the interaction representation.[12] In analogy with the closed-shell theory, we now introduce the quantities S_{ij} defined as follows:

$$S_{ij}(t) = i \langle \Phi_i | \exp[-i(H - E_c)t] |\Psi_{jH}\rangle / \langle \Psi_j^0 | \Psi_{jH}\rangle , \tag{5}$$

whose one-sided Fourier transform is

$$S_{ij}(\omega) = \int_{-\infty}^0 dt \, S_{ij}(t) \, e^{i\omega t}$$

$$= \langle \Phi_i | \frac{1}{\omega + E_c - H} |\Psi_{jH}\rangle / \langle \Psi_j^0 | \Psi_{jH}\rangle . \tag{6}$$

Clearly, $S_{ij}(\omega)$ has poles at $\omega = E_j - E_c$, which give the energy shift relative to the *exact* vacuum energy E_c. Our objective is to derive a perturbation expansion for $\mathbf{S}(t) = \{S_{ij}(t)\}$ and to obtain a Dyson-like equation for $\mathbf{S}$ from which we can compute the poles of $\mathbf{S}$. Using the Gellman–Low theorem [Eq. (4)], we have

$$S_{ij} = \frac{i\langle \Phi_i | \exp(-iH_0 t) \exp(iH_0 t) \exp[-i(H - E_c)t] U_I(0, -\infty) |\Psi_j^0\rangle}{\langle \Psi_j^0 | U_I(0, -\infty) |\Psi_j^0\rangle}$$

$$= i \frac{\exp[i(E_c - E_i^0)t] \langle \Phi_i | U_I(t, -\infty) |\Psi_j^0\rangle}{\langle \Psi_j^0 | U_I(0, -\infty) |\Psi_j^0\rangle}$$

$$\equiv N_{ij}/D_j . \tag{7}$$

Since the denominator D_j does not involve t as a variable, it does not affect the pole structure of $S_{ij}(t)$. We need therefore consider only the numerator N_{ij}.

Using the perturbation expansion[2] of $U_I(t, -\infty)$, the numerator N_{ij} can be written as

$$N_{ij}(t) = i \exp[i(E_c - E_i^0)t] \sum_{n=0}^\infty \frac{(-i)^n}{n!} \int_{-\infty}^t dt_1 dt_2 \cdots dt_n \langle \Phi_i | T[V_I(t_1) V_I(t_2) \cdots V_I(t_n)] |\Psi_j^0\rangle . \tag{8}$$

To facilitate further discussion it will be convenient to view the set of hole-particle creation operators in $\{\Omega_K^+\}$ as *valence* creation operators. We can then expand the time-ordered (T) product $T[\ ]$ in Eq. (8) in normal order using Wick's theorem,[2] taking Φ as the vacuum.

A typical term in Eq. (8) that needs to be evaluated is of the form $\langle \Phi | \Omega_i T[\ ] \Omega_K^+ | \Phi \rangle$, where $\Omega_K^+ | \Phi \rangle = \Phi_k$ arises from

the expansion of Ψ_j^0 according to Eq. (3). A typical term in the expansion of $T[\ ]$, using Wick's theorem, consists of a normal product of disjoint strings of operators $V_I(t_i) \cdots V_I(t_k)$, where in each string the operator V_I is joined to the rest of the string by at least one contraction. Since the matrix elements $\langle \Phi | \Omega_i N[\ ] \Omega_k^* | \Phi \rangle$ are to be evaluated as vacuum expectation values, they must consist of *completely contracted* terms and, hence, the leftover uncontracted operators in $N[\ ]$ must be fully contracted with the operators in Ω_i and Ω_k^* to give nonzero values. Because Ω_i and Ω_k^* contain *valence* operators only, the leftover uncontracted operators in $N[\ ]$ giving nonzero contribution to Eq. (8) must be *valence* operators only. In diagrammatic language, the normal products $N[\ ]$ giving nonzero contributions would thus correspond to disjoint strings with open lines (i.e., uncontracted operators) labeled by valence indices only. A closed *block* corresponds to a string in which *all* operators are completely contracted. Figure 1 shows a typical term $N[\ ]$ of Eq. (8).

Note that according to Eq. (8) all the intermediate time variables are to be integrated over the interval $(-\infty, t)$. We may classify the terms of Eq. (8) using the following device. For a given time ordering of the *open blocks*, we collect all possible time orderings of the closed blocks. We then consider all possible time orderings of such open blocks. This recipe clearly exhausts all of the terms in $T[\ ]$ of Eq. (8). For example, Fig. 1 shows one possible time ordering of the open blocks involving t_1, t_2, t_3, t_4, for which the contribution to N_{ij} of Eq. (8) is

$$N_{ij}^{(8')}(t) = i \exp[i(E_c - E_0^i)t](-i)^4 \int_{-\infty}^{t} dt_1 \int_{-\infty}^{t_1} dt_2 \int_{-\infty}^{t_2} dt_3 \int_{-\infty}^{t_3} dt_4 \langle \Phi_i | V_I(t_1)V_I(t_2)V_I(t_3)V_I(t_4) | \Psi_j^0 \rangle_{\text{open}}$$

$$\times \left\{ \frac{(-i)^4}{4!} \int_{-\infty}^{t} dt_5 \, dt_6 \, dt_7 \, dt_8 \langle \Phi | T[V_I(t_5)V_I(t_6)V_I(t_7)V_I(t_8)] | \Phi \rangle \right\} . \tag{9}$$

In writing this expression, we made use of the fact that the closed-block terms involving t_5, t_6, t_7, t_8 contain only completely contracted (cc) operators, so that

$$N[V_I(t_5)V_I(t_6)V_I(t_7)V_I(t_8)]_{\text{cc}} = \langle \Phi | T[V_I(t_5)V_I(t_6)V_I(t_7)V_I(t_8)] | \Phi \rangle .$$

Note that the contribution from the closed blocks, which is written within the curly brackets $\{\ \}$ of Eq. (9), is precisely one of the fourth-order terms of the $N(t)$ which appeared in our closed-shell theory [see Eq. (11) of I]. Thus, the complete expression for $N_{ij}(t)$, corresponding to all possible time orderings among all the open blocks for all of the closed blocks, has the form

$$N_{ij}(t) = i \sum_{m=0}^{\infty} \frac{(-i)^m}{m!} \exp[i(E_c - E_0^i)t] \int_{-\infty}^{t} dt_1 \cdots \int_{-\infty}^{t} dt_m \langle \Phi_i | T[V_I(t_1) \cdots V_I(t_m)] | \Psi_j^0 \rangle_{\text{open}} \frac{1}{i} N^{\text{closed}}(t) . \tag{10}$$

The value of $N^{\text{closed}}(t)$, given in Eq. (4) of I as $i \exp[(E_0 - E_c)t]\langle \Phi | \Psi \rangle$, then allows us to eliminate the *exact* vacuum energy E_c from Eq. (10) and obtain

$$N_{ij}(t) = i \sum_{m=0}^{\infty} \frac{(-i)^m}{m!} \exp[i(E_0 - E_0^i)t] \int_{-\infty}^{t} dt_1 \cdots \int_{-\infty}^{t} dt_m \langle \Phi_i | T[V_I(t_1) \cdots V_I(t_m)] | \Psi_j^0 \rangle_{\text{open}} \langle \Phi | \Psi \rangle$$

$$\equiv N_{ij}^{\text{open}}(t)\langle \Phi | \Psi \rangle . \tag{11}$$

Thus the factorization of N_{ij} into an open part times $N^{\text{closed}}(t)$ ensures that the correlated energy E_c of the vacuum drops out of the expression for $N_{ij}(t)$. Since $\langle \Phi | \Psi \rangle$ does not contribute to the poles of $N_{ij}(t)$, we can proceed to analyze $N_{ij}^{\text{open}}(t)$ only, which contains all of the desired pole information. The one-sided Fourier transform of $N_{ij}^{\text{open}}(t)$ has the form

$$N_{ij}^{\text{open}}(\omega) = i \sum_{m=0}^{\infty} \frac{(-i)^m}{m!} \int_{-\infty}^{0} dt \exp[i(\omega + E_0 - E_0^i)t] \int_{-\infty}^{t} dt_1 \cdots \int_{-\infty}^{t} dt_m \langle \Phi_i | T[V_I(t_1) \cdots V_I(t_m)] | \Psi_j^0 \rangle_{\text{open}} . \tag{12}$$

Following the lead given by the closed-shell case, our next objective is to write the above terms of $N_{ij}^{\text{open}}(\omega)$ in such a manner that the terms can be regrouped into a Dyson-like equation. Such regroupings are by no means unique. As we shall demonstrate below, the BW and RS perturbation series can be generated from two particular groupings. To facilitate the discussion of these theories, we introduce the concept of a "box." A box is a part of a diagram which cannot be further subdivided into two subboxes joined by *valence lines only*. As should become clear shortly, the boxes play the same role in our open-shell theory as the closed diagrams of the closed-shell theory of paper I. We also introduce a "string," which is a connected set of boxes joined by valence lines only. An open diagram of Eq. (12) will thus consist of a set of disjoint strings.

III. RESOLVENT THEORY: BW FORM

The expansion for $N_{ij}^{\text{open}}(\omega)$ given in Eq. (12) can be written in normal order as

$$N_{ij}^{\text{open}}(\omega) = i \sum_{m=0}^{\infty} (-i)^m \int_{-\infty}^{0} dt \exp[i(\omega + E_0 - E_0^i)t] \int_{-\infty}^{t} dt_1 \cdots \int_{-\infty}^{t_{m-1}} dt_m \sum_K \langle \Phi_i | N[Z_K(m)] | \Psi_j^0 \rangle_{\text{open}} , \tag{13}$$

where $\sum_K N[Z_K(m)]$ are the terms from the Wick theorem expansion of $T[V_I(t_1) \cdots V_I(t_m)] \equiv T[Z(m)]$ which gives nonvanishing contractions when sandwiched between $\langle \Phi | \Omega_i$ and $\Omega_K^* | \Phi \rangle$. Figure 2 shows a "box representation" of a typi-

cal term $Z_K(m)$. We first find the uppermost time level t_i lying below the highest time t_1 ($\leq t$) such that a horizontal cut at t_i cuts only the *valence* lines (i.e., the cut at t_i does not go through a box). This step is an exact analog of the one adopted in the earlier closed-shell BW theory (I). The set of boxes between t_1 and t_i will be called the "top part" and the remaining boxes below t_i the "bottom part." If we refer to the top part as X and the bottom part as Y, we show in Fig. 2 a particular connection (contraction) between X and Y. If one considers the set of diagrams arising from all possible connections (including no connection) between

$$N[XY] + N[\overparen{XY}] = T[XY] = T[X]T[Y] , \tag{14}$$

where $N[\overparen{XY}]$ denotes all possible contractions between X and Y and $N[XY]$ is the term having no contraction.

The first equality in Eq. (14) follows from Wick's theorem and the second equality follows because, by construction, all times in X are greater than all times in Y. It is clear from Fig. 2 that, for a given top part X, the collection of *all* possible bottom parts Y would be $\sum_l T[Z(l)]$, which is the same operator as appears in Eq. (13). Since all possible top parts exhaust all terms of $N_{ij}^{(\text{open})}$, we can write

$$N_{ij}^{(\text{open})}(\omega) = i \int_{-\infty}^{0} dt \exp[i(\omega + E_0 - E_0^i)t]\langle \Phi_i | \Psi_j^0\rangle + i \sum_{l=1}^{\infty} \sum_{m=0}^{\infty} (-i)^l(-i)^m \int_{-\infty}^{0} dt$$
$$\times \exp[i(\omega + E_0 - E_0^i)t] \int_{-\infty}^{t} dt_1 \cdots \int_{-\infty}^{t_{l-1}} dt_l \int_{-\infty}^{t_l} dt_{l+1} \cdots \int_{-\infty}^{t_{l+m-1}} dt_{l+m} \langle \Phi_i | T[X(l)]T[Z(m)]|\Psi_j^0\rangle_{\text{open}} , \tag{15}$$

where the first term is just the $m = 0$ term of Eq. (13). Introducing a resolution of identity $1 = \sum_i |\Phi_i\rangle\langle\Phi_i| + \sum_j |\bar{\Phi}_j\rangle\langle\bar{\Phi}_j|$, where $\bar{\Phi}_j$ are the eigenstates of H_0 lying *outside* the model space, and noting that $\langle\Phi_i|T[X(l)]|\bar{\Phi}_j\rangle \equiv 0$, since $X(l)$ contains only valence creation and annihilation operators, we have

$$\langle \Phi_i | T[X(l)]T[Z(m)]|\Psi_j^0\rangle_{\text{open}} = \sum_k \langle\Phi_i|T[X(l)]|\Phi_k\rangle\langle\Phi_k|T[Z(m)]|\Psi_j^0\rangle . \tag{16}$$

Thus, we have

$$N_{ij}^{\text{open}} = i \int_{-\infty}^{0} dt \exp[i(\omega + E_0 - E_0^i)t]\langle\Phi_i|\Psi_j^0\rangle + \sum_k \left(\left\{ \sum_{l=1}^{\infty} (-i)^l(-i)^m \int_{-\infty}^{0} dt \exp[i(\omega + E_0 - E_0^i)t] \right. \right.$$
$$\left. \left. \times \int_{-\infty}^{t} dt_1 \cdots \int_{-\infty}^{t_{l-1}} dt_l \int_{-\infty}^{t_l} dt_{l+1} \cdots \int_{-\infty}^{t_{l+m-1}} dt_{l+m} \langle\Phi_i|T[X(l)]|\Phi_k\rangle\langle\Phi_k|T[Z(m)]|\Psi_j^0\rangle_{\text{open}} \right\} \right) . \tag{17}$$

Equation (17) can be rewritten as

$$N_{ij}^{\text{open}}(\omega) = i \int_{-\infty}^{0} dt \exp[i(\omega + E_0 - E_0^i)t]\langle\Phi_i|\Psi_j^0\rangle + \sum_k \left(\left\{ \sum_{l=1}^{\infty} (-i)^l \int_{0}^{\infty} d(t - t_1) \exp[i(\omega + E_0 - E_0^i)(t - t_1)] \right. \right.$$
$$\left. \times \int_{-\infty}^{t} dt_1 \cdots \int_{-\infty}^{t_{l-2}} dt_{l-1} \exp[i(\omega + E_0 - E_0^i)t_1] \exp[-i(\omega + E_0 - E_0^k)t_l]\langle\Phi_i|T[X(l)]|\Phi_k\rangle_{\text{open,top}} \right\}$$
$$\left. \times \left\{ i \sum_{m=0}^{\infty}(-i)^m \int_{-\infty}^{t_{l-1}} dt_l \exp[i(\omega + E_0 - E_0^k)t_l] \int_{-\infty}^{t_l} dt_{l+1} \cdots \int_{-\infty}^{t_{l+m-1}} dt_{l+m} \langle\Phi_K|T[Z(m)]|\Psi_j^0\rangle_{\text{open}} \right\} \right) . \tag{18}$$

We can simplify the expression in the first curly bracket $\{ \}$ of Eq. (18) containing $X(l)$ by making use of the following facts.

(i) Any pair of contracted operators in $X(l)$ inside the boxes of the top part (see Fig. 2) between time vertices t_i and t_j contributes a factor of the form $\exp[iW(t_i - t_j)]$, where W involves orbital energy differences $(\sum W_h - \sum W_p)$.

(ii) The leftover uncontracted operators (corresponding to the open lines of the boxes in the top part) which ought to be contracted with the Ω_i and Ω_K^+ operators of $\langle\Phi_i| = \langle\Phi|\Omega_i$ and $|\Phi_k\rangle = \Omega_k^+|\Phi\rangle$), contribute factors $\exp[i(E_0^i - E_0)t_1]$ and $\exp[-i(E_0^K - E_0)t_l]$ which exactly cancel the $\exp[i(E_0 - E_0^i)t_1]$ and $\exp[-i(E_0^K - E_0)t_l]$ factors within the first curly bracket.

(iii) To facilitate time integrations, we can transform the time variables $t_1, t_2, \ldots, t_{l-1}$ to $(t_1 - t_2), (t_2 - t_3), \ldots, (t_{l-1} - t_l)$ with limits $(0, \infty)$. In terms of these time variables, we write the exponential factors as

$$\exp[iW(t_i - t_j)] = \exp\{iW[(t_i - t_{i+1}) + (t_{i+1} - t_{i+2}) + \cdots + (t_{j-1} - t_j)]\} . \tag{19}$$

(iv) With the above change of time variables, we can set the upper limit t_i in the second curly bracket equal to zero. We then immediately note that the expression in the second curly bracket is just $N_{kj}^{\text{open}}(\omega)$.

Using these manipulations, the expression for $N_{ij}^{\text{open}}(\omega)$ of Eq. (18) can be rewritten as follows:

$$N_{ij}^{\text{open}}(\omega) = \frac{1}{(\omega + E_0 - E_0^i)}\langle\Phi_i|\Psi_j^0\rangle + \sum_k \left\{ \left[\frac{1}{(\omega + E_0 - E_0^i)} \sum_{l=1}^{\infty}(-i)^{l-1} \int_{0}^{\infty} d(t_1 - t_2) \right. \right.$$
$$\left. \left. \times \exp[i(W_1 + \omega)(t_1 - t_2)] \cdots \int_{0}^{\infty} d(t_{l-1} - t_l) \exp[i(W_{l+1} + \omega)(t_{l-1} - t_l)]\langle\Phi_i|\underbrace{V \cdots V}_{\substack{l \\ \text{terms}}}|\Phi_k\rangle_{\text{open,top}} \right] [N_{kj}^{\text{open}}(\omega)] \right\} . \tag{20}$$

Here the factors W_i's are the sum over all W's arising from Eq. (19) with a common factor $(t_i - t_{i+1})$. To write Eq. (20) in a more compact form, we define the following quantities:

$$\overline{N}_{0,ij}^{\text{open}} \equiv [1/(\omega + E_0 - E_0^t)]\delta_{ij} \, , \tag{21}$$

$$N_{0,ij}^{\text{open}} = [1/(\omega + E_0 - E_0^t)]\langle \Phi_i | \Psi_j^0 \rangle \, , \tag{22}$$

$$\Sigma_{ik}^{\text{BW}}(\omega) = \sum_{i=1}^{\infty}(-i)^{(i-1)} \int_0^{\infty} d(t_1 - t_2) \exp[i(W_1 + \omega)(t_1 - t_2)]$$

$$\times \int_0^{\infty} d(t_{i-1} - t_i) \exp[i(W_{i-1} + \omega)(t_{i-1} - t_i)]\langle \Phi_i | V \cdots (l-\text{times}) \cdots V | \Phi_k \rangle_{\text{open,top}} \, . \tag{23}$$

Now Eq. (20) can be written as

$$N_{ij}^{\text{open}}(\omega) = N_{0,ij}^{\text{open}}(\omega) + \sum_k \overline{N}_{0,ii}^{\text{open}}(\omega)\Sigma_{ik}^{(\text{BW})}(\omega)N_{kj}^{\text{open}}(\omega) \, . \tag{24}$$

Multiplying by N^{closed}/D_j [see Eqs. (7) and (10)], we have

$$S_{ij}(\omega) = S_{0,ij}(\omega) + \sum_k N_{0,ii}^{\text{open}}\Sigma_{ik}^{\text{BW}}(\omega)S_{kj}(\omega) \, . \tag{25}$$

Equation (24) in matrix form reads

$$\mathbf{N}^{\text{open}}(\omega) = \mathbf{N}_0^{\text{open}}(\omega) + \overline{\mathbf{N}}_0^{\text{open}}(\omega)\Sigma^{\text{BW}}(\omega)\mathbf{N}^{\text{open}}(\omega) \, . \tag{26}$$

Equation (26) is a Dyson-like equation, from which, in principle, the poles of $\mathbf{N}^{\text{open}}(\omega)$ [or, equivalently, of $\mathbf{S}(\omega)$] can be obtained. However, this form of the equation seems to require explicit knowledge of Ψ^0 [through Eq. (22)] or of the coefficients C_{ij} [through Eq. (3)]. However, we now show that explicit knowledge of the coefficients c_{ij} is *not* required to obtain the poles of $\mathbf{N}^{\text{open}}(\omega)$. Using $\Psi_j^0 = \sum_i C_{ij}\Phi_i$ from Eq. (3) in Eq. (26) and defining

$$\overline{N}_{ij}^{\text{open}}(\omega) = i\sum_{m=0}^{\infty}\frac{(-i)^m}{m!}\int_{-\infty}^0 dt \exp[i(\omega + E_0 - E_0^t)t]\int_{-\infty}^t dt_1 \cdots \int_{\infty}^t dt_m \langle \Phi_i | T[V_I(t_1) \cdots V_I(t_m)] | \Phi_j \rangle_{\text{open}} \, , \tag{27}$$

Eq. (26) becomes

$$\overline{\mathbf{N}}^{\text{open}}(\omega)\mathbf{C} = \overline{\mathbf{N}}_0^{\text{open}}(\omega)\mathbf{C} + \overline{\mathbf{N}}_0^{\text{open}}(\omega)\Sigma^{\text{BW}}(\omega)\overline{\mathbf{N}}^{\text{open}}(\omega)\mathbf{C} \tag{28}$$

or, for $\mathbf{C}$ nonsingular,

$$\overline{\mathbf{N}}^{\text{open}}(\omega) = \overline{\mathbf{N}}_0^{\text{open}}(\omega) + \overline{\mathbf{N}}_0^{\text{open}}(\omega)\Sigma^{(\text{BW})}(\omega)\overline{\mathbf{N}}^{\text{open}}(\omega) \, . \tag{29}$$

Notice that now all quantities have been expressed in terms of the model space functions of $\{\Phi_i\}$ only. In practice, the poles of $\overline{\mathbf{N}}^{\text{open}}(\omega)$ are calculated as zeros of $\overline{\mathbf{N}}^{\text{open}}(\omega)^{-1}$ which can be expressed as

$$\overline{\mathbf{N}}^{\text{open}}(\omega)^{-1} = \overline{\mathbf{N}}_0^{\text{open}}(\omega)^{-1} - \Sigma^{\text{BW}}(\omega) \, . \tag{30}$$

Thus, zeroes of $\overline{\mathbf{N}}^{\text{open}}(\omega)^{-1}$ occur at values of ω satisfying (for nonvanishing amplitudes $\mathbf{A}$) an ω-dependent eigenvalue problem

$$[\overline{\mathbf{N}}_0^{\text{open}}(\omega)^{-1} - \Sigma^{\text{BW}}(\omega)]\mathbf{A} = 0 \, . \tag{31}$$

Using the fact [see Eq. (6)] that zeros of $\overline{\mathbf{N}}^{\text{open}}(\omega)^{-1}$ occur at $\omega = E_j - E_c$, and substituting Eq. (21) for $\overline{\mathbf{N}}_0^{\text{open}}$, we have

$$\omega A_j = [(E_0^j - E_c)\mathbf{1} + \Sigma^{\text{BW}}(\omega)]A_j \, . \tag{32}$$

The roots ω of Eq. (32) give the required energy shifts relative to vacuum's *exact* energy E_c. Thus the interpretation of the energy shift depends on the choices of Φ and $\{\Omega_i^*\}$. For example, if $\Phi = \Phi_{\text{HF}}$ for n electrons and if the operators $\{\Omega_i^*\}$ are taken to be single-electron attachment (or detachment) operators, $E_j - E_c$ would yield the corresponding attachment (or detachment) energies relative to the *exact* ground state of the n-electron system (i.e., the E.A.'s or I.P.'s of the system). On the other hand, if the $\{\Omega_i^*\}$ are excitation operators, one obtains the excitation energies relative to the n-electron *exact* ground state.

To make our discussion more concrete, let us take an example of a typical fourth-order diagram (Fig. 3) of Σ^{BW} occurring in an excitation energy calculation with vacuum as Φ_{HF} and $\{\Omega_i^*\}$ as $\{a_p^* a_\alpha\}$. Using the Goldstone diagrammatic rules,[15] we have

$$\Sigma_{p\alpha, r\beta}^{(4)}(\omega) = -\frac{1}{2^4}\sum_{\gamma,\delta,p,\lambda,k,l,m}\frac{\langle p\lambda | kl \rangle_a \langle kl | \lambda\gamma \rangle_a \langle \gamma\delta | m\alpha \rangle_a \langle m\beta | \gamma\delta \rangle_a}{(\omega + \epsilon_\lambda + \epsilon_\alpha - \epsilon_k - \epsilon_l)(\omega + \epsilon_\lambda + \epsilon_\gamma + \epsilon_\delta - \epsilon_k - \epsilon_l - \epsilon_m)(\omega + \epsilon_\gamma + \epsilon_\delta - \epsilon_\gamma - \epsilon_m)} \, . \tag{33}$$

This is precisely a fourth-order term in the open-shell BW perturbation theory in the form derived by Bloch and Horowitz (BH) (1958).[3] We may note here three

characteristic features of the BH perturbation theory: (i) the appearance of $(E_j - E_c)$, the energy shift relative to the exact vacuum energy E_c in the denominators of
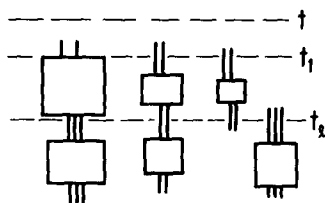
FIG. 2. "Box representation" of a typical term in the expansion of N_{ij}^{open} [Eq. (13)]. t_1 is the topmost time argument in the entire diagram. t_l is the uppermost time level below t_1 such that a horizontal line drawn at t_l cuts valence lines only. The portion of the diagram between t_1 and t_l is the "top" part and the rest is the "bottom" part of the diagram.

Σ; (ii) the appearance of mutually overlapping disconnected open diagrams; and (iii) the absence of closed diagrams. In contrast, in the conventional open-shell BW perturbation theory[16] the calculated energy shifts $(E_j - E_j^0)$ are given relative to the *unperturbed* energies E_j^0. In our derivation this change can be effected by a simple substitution of E_c by E_j^0 in Eq. (5). This ease of interconversion stands in contrast to the time-independent derivations of, for example, BH,[3] and Brandow,[4,10] where a great deal of "juggling" of energy denominators is required to achieve this reduction.

The key points of our development can be summarized as follows. In the perturbation expansion of S, contributions from its closed diagrams were shown to factor out [Eq. (10)]. Secondly, the set of open diagrams can be regrouped to appear as Σ S, where Σ contains a set of mutually overlapping disconnected diagrams containing only open valence lines. This regrouping leads to a Dyson-like equation for S. Moreover, a knowledge of the combining coefficients C is not required for calculation of the poles of S.

Since, in our development, the poles of S appear at the energy differences $E_j - E_c$, the state energies E_j may be calculated by adding the value E_c to the poles $E_j - E_c$ of S. Since the vacuum Φ is a closed shell, E_c can be calculated from the closed-shell perturbation theory (I).

As found earlier for the closed-shell problem, the BH (or BW) open-shell MBPT gives rise to diagrams such as that shown in Fig. 3 (when each disconnected part contains orbital indices corresponding entirely to fragments f_1 and f_2) and yields an energy of the form $E_{f1} E_{f2}$ which, at dissociation, remains nonvanishing. Thus, this open-shell BW theory is not size-consistent.

IV. TREATMENT OF QUASIDEGENERACY

In real situations one rarely encounters *exactly* degenerate model space functions. In general, one has only nondegenerate orbitals in the model space and hence nondegenerate $\{\Phi_i\}$ with respect to the unperturbed Hamiltonian. For example, it is customary and convenient to construct the set $\{\Phi_i\}$ from the set of Hartree-Fock (HF) orbitals, which are nondegenerate with respect to the Fock operator f. These Φ_i's satisfy

$$F\,\Phi_i = \tilde{E}_0^i \Phi_i \ , \tag{34}$$

where $F = \sum_i f(i)$. In formulating a useful MBPT, it would be desirable to choose F as the unperturbed Hamiltonian and $V' = H - F$ as the perturbation. In order to show how the above choice of a Fock-operator-based unperturbed Hamiltonian with nondegenerate model space functions may be made consistent with the development given earlier, we proceed in two steps.

In the first step we show that starting with nondegenerate $\{\Phi_i\}$ it is always possible to choose a one-electron operator H_0 which restores the degeneracy of the $\{\Phi_i\}$, with

$$H_0 = F + Z \ . \tag{35}$$

Then our earlier development of the theory carries through with the perturbation V given by

$$V = H - F - Z = V' - Z \ . \tag{36}$$

To establish the form of the operator Z, we designate by χ_i^c and χ_i^v, respectively, the vacuum and valence orbitals in the model space which are eigenfunctions of some one-body operator f:

$$f\chi_i^c = \epsilon_i^c \chi_i^c \tag{37}$$

and

$$f\chi_i^v = \epsilon_i^v \chi_i^v \ . \tag{38}$$

Then a one-electron operator h_0 defined in terms of the valence-orbital projectors $|\chi_i^v\rangle\langle\chi_i^v|$ and as yet undetermined amplitudes z_i^v,

$$h_0 = f + z = f + \sum_i |\chi_i^v\rangle\langle\chi_i^v| z_i^v \ , \tag{39}$$

has the property that

$$h_0 \chi_i^c = \epsilon_i^c \chi_i^c \tag{40}$$

and

$$h_0 \chi_i^v = (\epsilon_i^v + z_i^v) \chi_i^v \ . \tag{41}$$

Thus a choice of the amplitudes z_i^v as

$$z_i^v = \epsilon^v - \epsilon_i^v \tag{42}$$

for any arbitrary *constant* ϵ^v, leads to an *exact* degeneracy of the orbitals χ_i^v with respect to h_0 with an eigenvalue ϵ^v. The model space functions $\{\Phi_i\}$ would therefore be degenerate with respect to the operator
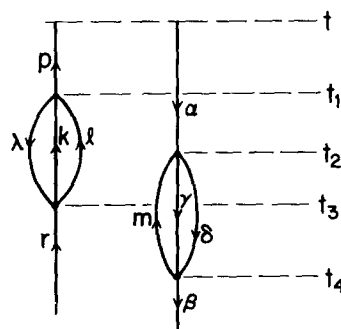

FIG. 3. A typical disconnected open diagram contributing to Σ_{BW} in the open-shell BW theory. This kind of diagram renders the BW theory size-inconsistent.

$$H_0 = \sum_i h_0(i) = F + Z \ , \tag{43}$$

with Z given by

$$Z = \sum_{i \in v} z_i^v a_{i_I}^+ a_{i_I} \ . \tag{44}$$

The degenerate eigenvalues E_0^i of Φ_i satisfy

$$H_0 \Phi_i = E_0^i \Phi_i \ , \tag{45}$$

where

$$E_0^i = \sum_{i \in \Phi_0} \epsilon_i^c + n\epsilon^v \tag{46}$$

and n is the number of valence orbitals in each Φ_i.
Notice that Z of Eq. (44) is a diagonal one-body operator.

In the second step of our treatment of the nondegenerate case, we *undo* the effect of degeneracy brought about through Z by summing all the terms in the perturbation series [Eq. (27)] to infinite order in $-Z$. The degenerate unperturbed energies E_0^i then become shifted, *as a consequence of the infinite summation*, to the corresponding eigenvalues $\bar{E}_0^i$ of F. Moreover, in the energy denominators the orbital energies ϵ^v for the valence orbital χ_i^v get shifted to ϵ_i^v, the eigenvalues with respect to f. The remaining part of the perturbation V' appearing in Eq. (36) can then be treated order by order. The details of this infinite summation scheme have been described in Appendix A. Here we simply summarize the results. The net effect of the resummation is a perturbation theory with F as the unperturbed Hamiltonian and V' as the perturbation. The model space functions $\{\Phi_i\}$ are *no longer degenerate* with respect to this partition, but the results in Sec. III still hold.

Hence, in the next section, where we develop the resolvent theory in the RS form, we can assume that the $\{\Phi_i\}$ may not be degenerate.

V. RESOLVENT THEORY: RS FORM

Let us recall the procedure used in the closed-shell RS case to break $N(t)$ into top and bottom parts. The top part corresponded to the closed, connected diagrams involving the highest time vertex and was identified as Σ; the bottom part was identified with N. A straightforward application of this procedure to the open-shell case with the top box identified as the top part runs into difficulties. The problem is that factorization analogous to Eq. (14) (i.e., $T[XY] = T[X]T[Y]$) cannot be obtained for open shells because the top part X and the bottom part Y generally involve uncontracted operators having overlapping time arguments. Even though the highest time in the top part X is above all time arguments in Y, a vertex in X where valence lines enter might have a
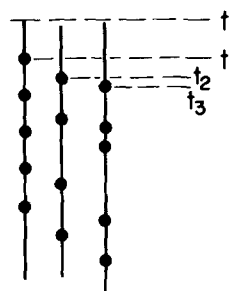

FIG. 4. Schematic representation of the series for N_{ij}^{open} in terms of a string of "pointlike" or instantaneous vertices, appropriate to generating the Σ_{RS} for open-shell RS theory. The point with the highest time argument t_1 in the entire diagram is the "top" part for RS theory; the rest is the bottom part. The diagram shown here has time arguments $t_1 > t_2 > t_3$, etc.

time argument less than one in Y (see Fig. 3). A technique, by no means unique, which allows us to overcome this problem and still effect such a factorization leading to an ω-independent Σ is given below.

If a box could be replaced by an equivalent "pointlike" or *instantaneous* vertex in which the valence lines enter and leave at the *same* time, then a string of boxes can be represented as a string of points. In other words, we intend to replace the true series of boxes in $\mathbf{N}^{\text{open}}$ by a model series containing points. A typical term $Z_K(m)$ of N_{ij}^{open}, as represented in terms of m pointlike vertices, is shown in Fig. 4:

$$N_{ij}^{\text{open}}(\omega) = i \sum_{m=0}^{\infty} \int_{-\infty}^{0} dt \, \exp[i(\omega + E_0 - E_0^i)t]$$
$$\times \int_{-\infty}^{t} dt_1 \cdots \int_{-\infty}^{t_{m-1}} dt_m \sum_K \langle \Phi_i | N[Z_K(m)] | \Psi_j^0 \rangle_{\text{open}} \ . \tag{47}$$

The sign factors like $(-1)^P$ have been incorporated into the point like Z_K's. If we now choose as the top part X the point labeled by time t_1, and the rest of the diagram as the bottom part Y, and consider all possible connections (diagrams) between X and Y, then the desired factorization immediately follows:

$$N[XY] + N[\overline{XY}] = T[XY] = X(t_1)T[Y] \ . \tag{48}$$

Note that all of the top parts X involve only the single time argument t_1. For a given top part X, the collection of all possible bottom parts Y would be $\sum_l \sum_K N[Z_K(l)]$ which is the same operator as that appearing in Eq. (47). Thus, this procedure, after all top parts X are considered, exhausts all the terms of N_{ij}^{open}.

Introducing now the resolution of identity $1 = \sum_l |\bar{\Phi}_j\rangle \times \langle \bar{\Phi}_j|$ and using a manipulation similar to the one adopted in the passage from Eqs. (15) to (20), we obtain

$$N_{ij}^{\text{open}}(\omega) = i \int_{-\infty}^{0} dt \, \exp[i(\omega + E_0 - E_0^i)t]\langle \Phi_i | \Psi_j^0 \rangle + \sum_k \left[\sum_x \int_0^{\infty} d(t - t_1) \exp[i(\omega + E_0 - E_0^i)t]\langle \Phi_i | X(t_1) | \Phi_K \rangle_{\text{open, top}} \right]$$
$$\times \exp[-i(\omega + E_0 - E_0^K)t_1] \sum_{m=0}^{\infty} \sum_L \int_{-\infty}^{0} dt_1 \, \exp[i(\omega + E_0 - E_0^K)t_1] \int_{-\infty}^{t_1} dt_2 \cdots \int_{-\infty}^{t_m} dt_{m+1} \langle \Phi_K | N[Z_L(m)] | \Psi_j^0 \rangle_{\text{open}} \ . \tag{49}$$

Let us note that $X(t_1)$ contains a normal product of creation and annihilation operators with the same time argument

t_1. The term $X(t_1)$ thus has the form $\exp(iH_0 t_1 X)\exp(-iH_0 t_1)$, where X is independent of time. Since $\langle\Phi_i|$ and $|\Phi_n\rangle$ are eigenstates of H_0 with eigenvalues E_0^i and E_0^K, we have

$$N_{ij}^{\text{open}}(\omega) = i\int_{-\infty}^{0} dt\, \exp[i(\omega + E_0 - E_0^i)t]\langle\Phi_i|\Psi_j^0\rangle + \sum_k \left[\sum_X \int_0^{\infty} d(t - t_1)\exp[i(\omega + E_0 - E_0^i)(t - t_1)]\langle\Phi_i|X|\Phi_K\rangle_{\text{open,top}}\right]$$

$$\times \sum_{m=0}^{\infty}\sum_L \int_{-\infty}^{0} dt_1 \exp[i(\omega + E_0 - E_0^K)t_1]\int_{-\infty}^{t_1} dt_2 \cdots \int_{-\infty}^{t_m} dt_{m+1}\langle\Phi_K|N[Z_L(m)]|\Psi_j^0\rangle_{\text{open}} \qquad (50)$$

or

$$N_{ij}^{\text{open}}(\omega) = N_{0,ij}^{\text{open}}(\omega) + \sum_k \overline{N}_{0,ii}^{\text{open}}(\omega)\Sigma_{ik}^{\text{RS}}N_{kj}^{\text{open}}(\omega)\ , \qquad (51)$$

which reads in matrix notation

$$\mathbf{N}^{\text{open}}(\omega) = \mathbf{N}_0^{\text{open}}(\omega) + \overline{\mathbf{N}}_0^{\text{open}}(\omega)\mathbf{\Sigma}^{\text{RS}}\mathbf{N}^{\text{open}}(\omega)\ , \qquad (52)$$

where $\overline{N}_{0,ij}^{\text{open}}$ and $N_{0,ij}^{\text{open}}$ are defined in Eqs. (21) and (22), respectively, and Σ_{ik}^{RS} is

$$\Sigma_{ik}^{\text{RS}} \equiv \sum_X \langle\Phi_i|X|\Phi_k\rangle_{\text{open,top}}\ . \qquad (53)$$

It should be noted here that Σ^{RS} in Eq. (52) is ω-independent by construction.

As was shown earlier in connection with the BW theory [see Eqs. (26)–(31)], calculation of poles of $\mathbf{N}^{\text{open}}(\omega)$ does *not* require explicit knowledge of coefficients C_{ij}. Using Eqs. (21) and (22) and eliminating **C**, we have

$$\overline{\mathbf{N}}^{\text{open}}(\omega) = \overline{\mathbf{N}}_0^{\text{open}}(\omega) + \overline{\mathbf{N}}_0^{\text{open}}(\omega)\mathbf{\Sigma}^{\text{RS}}\overline{\mathbf{N}}^{\text{open}}(\omega)\ . \qquad (54)$$

In practice, the poles of $\overline{\mathbf{N}}^{\text{open}}(\omega)$ will be calculated as the zero's of $\overline{\mathbf{N}}^{\text{open}}(\omega)^{-1}$, which occur for nonvanishing amplitudes A satisfying

$$[\overline{\mathbf{N}}_0^{\text{open}}(\omega)^{-1} - \mathbf{\Sigma}^{\text{RS}}]A = 0\ . \qquad (55)$$

Using Eq. (6) we have the eigenvalue equations

$$\omega A_j = [(E_0^j - E_0)\mathbf{1} + \mathbf{\Sigma}^{\text{RS}}]A_j\ , \qquad (56)$$

giving the required energy shifts as roots ω. Because $\mathbf{\Sigma}^{\text{RS}}$ is ω-independent, solution of Eq. (56) is noniterative for ω.

In contrast to the BW theory, the Σ in the RS theory consists of connected diagrams only. Thus, for two non-interacting fragments, the RS analog of the diagram of Fig. 3 would be connected leading to vanishing interaction at infinite separation of the fragments. As a result, the energy computed via the RS method is potentially size-consistent.

Although the above analysis shows how the RS version of the Dyson equation is obtained, it was predicated upon our ability to replace boxes by instantaneous point interactions. We now show, following Johnson and Baranger, [9] that such a replacement is indeed valid.

A. Johnson–Baranger method of folding diagrams

Our objective here is to explore the possibility of replacing boxes by equivalent "points" and that a string of boxes could be made equivalent to a string of points. Figure 5 demonstrates pictorially a procedure for achieving such a reduction. Figure 5(a) shows a typical box between the time ranges t_1 and t_2, with $t > t_1 > t_0 > t_2 > t'$, where t and t' are the times above and below which

the box connects with other boxes of the string. The time t_0 lies between t_1 and t_2 and is chosen to define the time corresponding to the instantaneous interaction for the "point." The time-dependent part of diagram 5(a) has the form

$$T \equiv \exp[iW_0(t - t_1)]$$

$$\times \{\exp[iW(t_1 - t_2)]\}\exp[iW_i(t_2 - t')]\ , \qquad (57)$$

where each W corresponds to an appropriate orbital energy difference $(\Sigma_h\epsilon_h - \Sigma_p\epsilon_p)$ between the respective time intervals. This expression can be rewritten as

$$T = \exp[iW_0(t - t_0)]\{\exp[-iW_0(t_1 - t_0)]\exp[iW(t_1 - t_2)]$$

$$\times \exp[-iW_i(t_0 - t_2)]\}\exp[iW_i(t_0 - t')]\ , \qquad (58)$$

which corresponds to the diagram 5(b). The quantity inside the curly brackets { } corresponds to the "folded" box which defines the "point" [Fig. 5(d)]. It is evident from Fig. (5) and the algebra expressed in Eq. (58) that the folded incoming and outgoing lines in the box [Fig. 5(e)] have arrows pointing in the opposite direction {corresponding to the exponential factors $\exp[-iW_i(t_0 - t_2)]$ and $\exp[-iW_0(t_1 - t_0)]$}. The introduction of these so-called folded lines[9] was necessary to nullify the effect of "stretching" the external incoming and outgoing lines of the original box to the point t_0. Clearly no such folding is required for a box whose incoming time lies above the outgoing time, as is illustrated in Fig. 6.
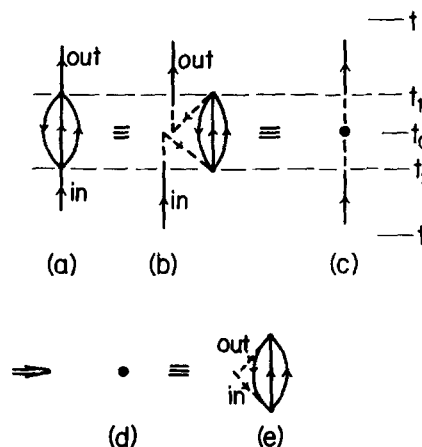
FIG. 5. Diagrammatic representation of the folding procedure of Johnson and Baranger. (a) shows a typical box with time arguments t_1 and t_2. (b) is the same box, but with external open lines stretched to a common time argument t_0 lying between t_1 and t_2. The stretched portions are shown with dotted lines. (c) shows how (b) may be viewed as a diagram with a pointlike interaction at t_0, shown separately in (d). (e) shows what the point is like. The dotted lines on the box in (e) correspond to "folded" lines.
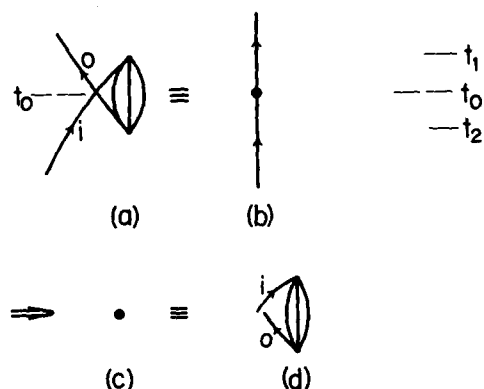
FIG. 6. For a box whose incoming time lies above the outgoing time, the conversion of the box to a point introduces no folded lines whatsoever. Figures (a) to (d) show such a conversion diagrammatically.
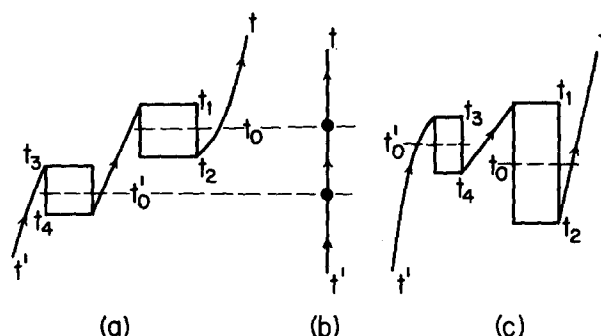

FIG. 8. Depiction of a situation where a string of boxes excludes a time range present in the true series containing boxes. (a) shows a true series with two boxes and (b) shows the corresponding model series containing two points. The true series requires $t > t_1 > t_2$, $t_3 > t_4 > t'$, $t_1 > t_4$. But the model series has a further restriction $t_0 > t_0'$. The model series thus excludes the range $t_0 < t_0'$. A true-correcting (TC) diagram shown in (e) must therefore be added to the model series of (b).

Further analysis shows that the above recipe for replacing a box by an equivalent point does *not* simply reduce a *string* of boxes to an equivalent string of points within the allowable time range unless correction terms are brought in. Figure 7(a) shows a string of two points obtained by replacing each box of the string of Fig. 7(b) by a point. The model series of Fig. 7(a) implies that $t > t_0 > t_0' > t'$ with $t_1 > t_0 > t_2$ and $t_3 > t_0' > t_4$. The *true* series of Fig. 7(b), however, requires $t > t_1 > t_2 > t_3 > t_4 > t'$. Thus the model series, which has no restriction on the relative ordering of t_2 and t_3, includes spurious contributions from the range $t_2 < t_3$ even though the model restriction $t_0 > t_0'$ still applies. Such spurious contributions, therefore, must be *subtracted* from the expression of the string of points for the desired equivalence

to hold. The spurious terms contained in the model string of points have the box structure shown in Fig. 7(c) and are called *model-correcting* (MC) diagrams.[9] It is evident from Fig. 7(c) that the MC term has intermediate valence line(s) running in directions opposite to their original direction in the true series [Fig. 7(b)] and thus appear as folded. Since the entering and leaving vertices [t_4 and t_1 in Fig. 7(c)] of such MC terms are, in general, unequal, these must be folded to a point for actual evaluation. {MC terms with multiply folded intermediate valence lines appear in (i) a string [Fig. 7(a)], in which one or more of the points originate from a term [Fig. 7(c)], or (ii) the string containing three or more points. For details see Ref. 9.}

In Fig. 8 we illustrate the other case in which a string of points *excludes* a time range present in the corresponding "true" string of boxes. The true series [Fig. 8(a)] requires $t > t_1 > t_2$, $t_3 > t_4 > t'$, and $t_1 > t_4$, while the model series [Fig. 8(b)] has $t_1 > t_0 > t_2$, $t_3 > t_0' > t_4$, and $t_0 > t_0'$. Thus the model description *excludes* the time range in which $t_0 > t_0'$. A *"true-correcting"*[9] (TC) diagram, as shown in Fig. 8(c), should therefore be *added* to the expression of the model series of Fig. 8(b). As with the MC terms, the TC terms are to be folded to a point for their evaluation. In addition, there exist boxes of the true series in which the entering and leaving lines emerge from the same vertex and are thus automatically pointlike.[13]

Thus far we have not specifically discussed any procedure for choosing the folding time t_0 defining the point interaction. Following JB,[9] we chose t_0 to be *midway* between the incoming and outgoing vertices of a box diagram to ensure the Hermiticity of the resulting Σ^{RS}. In Appendix B we discuss further the details of the time integration procedure for the calculation of folded boxes (points). Unlike the JB folding procedure, with our choice of boxes the internal holes and particles are treated symmetrically. Details for calculating the expressions for folded diagrams are given in Appendix B.

FIG. 7. Emergence of model correcting diagrams for a diagram having two boxes. (a) shows a string of two points obtained by replacing each box of the string shown in (b) by a point. The restriction on time arguments in the model series (a) is $t_0 > t_0'$, with t_0 and t_0' lying between t_1, t_2 and t_3, t_4, respectively. The true series has an additional restriction: $t_2 > t_3$. The model series (a) has thus a spurious contribution from the range $t_2 < t_3$, as shown in (c). Such contributions must, therefore, be subtracted from the expression for the string of points for the equivalence to hold. Such terms have been called model-correcting (MC) diagrams (see, e.g., Ref. 9). Note that as a result the line joining the boxes in Fig. 7(c) goes the "wrong way."

VI. RENORMALIZATION IN RS THEORY

In many applications of perturbation theories, it is customary to choose the HF orbitals for the ground state as the basis set for the calculations. The principal consequence of this choice is the absence of first-order diagrams in the one-body Σ. This comes about since the definition of the unperturbed Hamiltonian H_0 includes the effect of all such first-order diagrams through v_{HF}. To achieve a generalization of this concept, we intend to find a one-particle potential u which includes a desired set of diagrams to all orders appearing in Σ. Introduction of such a one-particle u in H_0 defines a partition of H:

$$H = H_0 + V , \tag{59}$$

$$H_0 = \langle \Phi | H | \Phi \rangle + \sum_i \epsilon_i N[a_i^+ a_i] , \tag{60}$$

where

$$H_0 = \sum_i h_0(i) = \sum_i [h(i) + u(i)] . \tag{61}$$

The orbitals χ_i are chosen to be eigenfunctions of h_0:

$$h_0 \chi_i = \epsilon_i \chi_i , \tag{62}$$

and the perturbation V is given by

$$V = \frac{1}{2^2} \sum_{ijkl} \langle ij | kl \rangle_a N[a_i^+ a_j^+ a_l a_k] + \sum_i [v_{HF}(i) - u(i)]$$

$$= G + \sum_i [v_{HF}(i) - u(i)] . \tag{63}$$

$v_{HF}(i)$ has the form of the HF potential and would reduce to the HF potential itself if HF orbitals are used. Since Σ is a power series in V, the diagrams in Σ will contain contributions from G, v_{HF} as well as u. If we want certain diagrams not to appear in Σ (i.e., their contribution should vanish) then we must choose u to achieve a cancellation between terms coming from G, v_{HF}, and u. This criterion then serves to define u.[19] We illustrate this procedure by first considering elimination of the first-order contributions in Σ, which leads to the choice $u = v_{HF}$. Although this is obvious from Eq. (63), we show this cancellation as a prelude to our treatment of the more general case.

Following the usual Goldstone convention, we designate the operator v_{HF} by a bubble, as shown in Fig. 9(a). We denote the one-particle potential u by a cross as in Fig. 9(b). Terms in Σ containing bubbles and crosses can be depicted as in Fig. 10, where typical diagrams up to second order have been displayed. The symbolic box contains the interactions from G, but contains no

(a)   (b)

FIG. 9. (a) Diagrammatic representation of the Hartree–Fock (HF) operator V_{HF} as a bubble; (b) a corresponding diagram for an external one-body potential u, denoted by a cross.
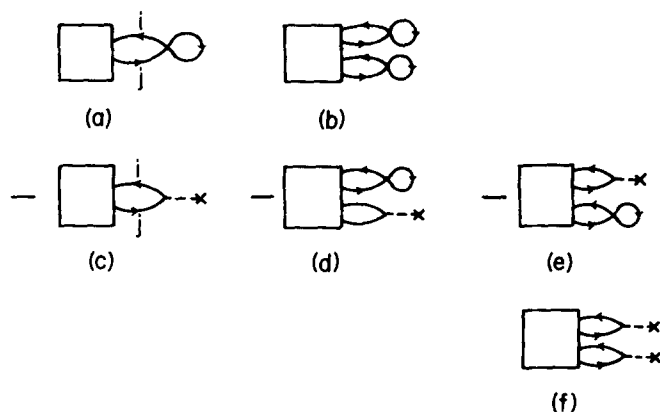
FIG. 10. Diagrammatic representation of all the terms having at most a total of two bubbles or crosses. The boxes shown here are defined as part of a diagram not containing any bubble or cross. If the cross is defined to have a value equal to that of the bubble, then [(a),(c)], [(b),(d)], and [(e),(f)] mutually cancel each other.

bubbles or crosses. The lines i, j need not necessarily be both connected to the box. In particular, when both i, j are open we have a "no box situation" in which case the bubble itself is a diagram of Σ. (Note that Σ contains connected diagrams only.) We take the labels (i,j) to be unrestricted (e.g., going over holes as well as particles) because we want to define u over the complete orbital space. Let us recall that v_{HF} is also defined over a complete orbital space. If we now assign to a cross a value equal to that of a bubble (with the rest of the box remaining the same), then [(a),(c)], [(b),(d)], and [(e),(f)] in Fig. 10 mutually cancel each other. Such cancellations can be shown to be true for higher order diagrams as well. For this particular type of cancellation to hold to all orders, we must have

$$u_{ij} = v_{HF,ij} = \sum_{\alpha \in \Phi} \langle i\alpha | j\alpha \rangle_a . \tag{64}$$

With this choice of u, h_0 becomes the HF operator from Eq. (61).

In general, u can be chosen to eliminate any desired set of diagrams in Σ. As an example, the elimination for the second-order diagrams is shown below. Since u is a function of the orbitals $\{\chi_i\}$, and since we choose to define the orbitals as eigenfunctions of h_0, Eq. (62) has to be solved self-consistently. We refer to such an iterative solution for u and $\{\chi_i\}$ as a renormalization procedure.

The principal implication of this renormalization is the absence of all diagrams in Σ which contain an interaction which we have chosen to eliminate through u. As an example, with the choice of HF orbitals (first-order renormalization) there would be no diagrams in Σ containing a bubble (i.e., there is no contribution from the Coulomb minus exchange interaction). For the orbitals $\{\chi_i\}$ to remain orthonormal, the self-consistent solution of Eq. (62) requires h_0 to be Hermitian. Thus u has to be an ω-independent and Hermitian operator. It is to be noted that the first-order renormalization leading to HF orbitals defines $u = v_{HF}$ as trivially ω-independent and
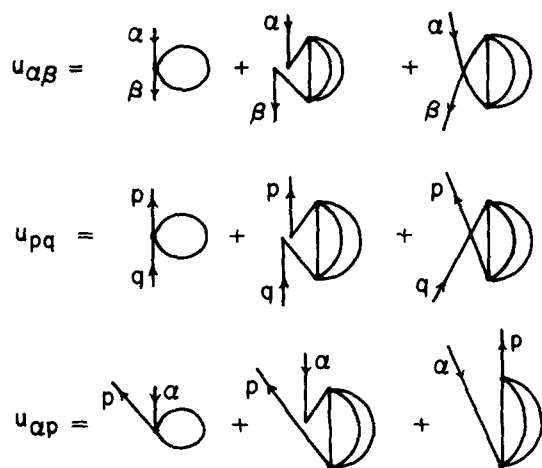
FIG. 11. Diagrammatic representation of all the terms contributing to u for a renormalization up to second order.

Hermitian. However, for a general u corresponding to a higher order renormalization, the diagrams defining u have to be folded to keep u ω-independent and Hermitian. As an example, we have listed in Fig. 11 all the folded skeletons of u for a renormalization up to second order.

VII. CONCLUDING REMARKS

In these first two articles we developed a unified time-dependent approach for treating closed- and open-shell perturbation theories in the RS and BW forms, starting from the resolvent of the Schrödinger equation. The underlying common feature for both the closed- and open-shell developments is the dissection of the perturbation series for the resolvent into appropriate "top" and "bottom" parts leading to Dyson-like equations involving the effective Hamiltonian Σ in RS as well as BW form. The highlights of this development for open shells can be summarized as follows. The energy shifts, calculated as poles of the resolvent in our theory, are obtained relative to the *correlated* vacuum energy. The explicit elimination of closed diagrams, corresponding to the vacuum's correlation energy, is achieved in a rather straightforward manner within our time-dependent framework. In the BW case, the ω-dependent effective Hamiltonian Σ contains mutually overlapping disconnected diagrams with only open valence lines. On the other hand, the Σ for the RS series contains only connected diagrams and thus leads to a size-consistent theory.

In the open-shell RS case, the effective Hamiltonian Σ was made ω-independent and Hermitian by using the time integration procedure of JB, who prescribed a recipe[9] for "folding" diagrams which converts a time-delayed interaction into a set of equivalent *instantaneous* interactions and also ensures Hermiticity of the instantaneous interaction. In the conventional MBPT theories for closed or open shells, the use of the Bruckner-Goldstone-type series for ΔE requires explicit cancellation of the disconnected diagrams common to the numerator and denominator. In contrast, in our approach it suffices to have a dissection of the series for the

resolvent in which such unwanted diagrams are contained in the bottom part.

It is appropriate here to comment briefly on the other existing resolvent-based perturbation theories. Hugenholtz,[17] Kvasnička,[5] and Bloch and Horowitz[3] made use of resolvents in their closed-[17] and open-shell[3,5] versions of MBPT in a time-independent framework. The elimination of disconnected diagrams in the closed-shell RS theory of Hugenholtz[17] and its open-shell generalization by Kvasnička,[5] and of the closed diagrams in the open-shell BW theory of Bloch and Horowitz, required considerable juggling of the energy denominators due to their time-independent approach. Löwdin[18] reformulated RS and BW perturbation theories using reduced resolvents. The series he generated were configuration-based rather than orbital-based, and are thus not immediately adaptable to the MBPT form. Johnson and Baranger[9] introduced quantities akin to our $S(t)$ in their time-dependent treatment of the open-shell RS theory, and their development is closest in spirit to our approach. The major highlight of their work is the "folding" idea discussed earlier. In our opinion, however, their general formal development beyond the folding idea is rather incomplete. In particular, their starting definition of the resolvent [Eq. (9) of Ref. 9] implies that the energy shifts are to be found relative to the *unperturbed* vacuum energy E_0. Thus a perturbation expansion of such a resolvent would have contained disconnected closed diagrams, whereas in our theory the presence of the correlated vacuum energy E_c in the resolvent ensures elimination of these terms. Recently, attempts have been made to generate Hermitian model Hamiltonians through Van Vleck unitary transformations.[19,20] The relations between several existing open-shell perturbation theories have also been recently explored.[21] With only one model space configuration, the formulations of Brandow,[4] Kvasnička[5] and ours become essentially the same.

In the following paper we apply the open-shell resolvent theory in the RS form for calculating the I.P.'s, E.A.'s, E.E.'s, and state energies of some prototype systems.

ACKNOWLEDGMENTS

APPENDIX A

In Sec. IV we discussed a procedure for treating nondegenerate Φ_i's in the model space in our perturbation theory. This goal was achieved in two steps. In the first step, we restored the degeneracy of the Φ_i's by adding a *one-body* operator Z to F to construct the H_0 ($H_0 = F + Z$) of Eq. (35). In this appendix we give the details of the second step where we exactly undo the effect of the inclusion of Z in H_0 by treating $-Z$ in the perturbation series to infinite order. Operationally speaking, we then have a perturbation theory in which

FIG. 12. Diagrammatic representation of the perturbation expansion of $\bar{N}_F^{0\,\text{open}}$ introduced in Eq. (A2) for a two-body Σ. The square vertex corresponds to the operator $-Z$, introduced in Eq. (35).

the model space functions $\{\Phi_i\}$ are nondegenerate with respect to an unperturbed Hamiltonian F and the perturbation is now $V' = H - F$ [Eq. (36)].

To begin our analysis, let us denote the perturbation $-Z$ in V by a square vertex. A resolvent $\bar{N}_F^0(t)$, defined with respect to the operator F, has the form

$$\bar{N}_{Fij}^0(t) = i\langle \Phi_i \,|\, \exp[-i(F - E_c)t] \,|\, \Phi_j \rangle \ . \tag{A1}$$

Its perturbation series with respect to the unperturbed Hamiltonian H_0 of Eq. (35) can be developed in a way analogous to Eq. (11), leading finally to a Dyson-like equation of the form of Eq. (26):

$$\bar{N}_F^{0\,\text{open}}(\omega) = \bar{N}^{0\,\text{open}}(\omega) + \bar{N}^{0\,\text{open}} \Sigma_Z^{BW} \bar{N}_F^{0\,\text{open}} \ , \tag{A2}$$

where Σ_Z^{BW} is just $-Z$, since Z is a *diagonal* one-body operator [see Eq. (44)] involving valence lines only. The expanded form of Eq. (A2) gives the series for $\bar{N}_F^{0\,\text{open}}$ in powers of Z, as shown in Fig. 12 for a two-body Σ. Thus, a collection of valence lines with an infinite number of $-Z$ insertions attached to all of them gives an element of $\bar{N}_F^{0\,\text{open}}$ in which the Hamiltonian that appears is F rather than H_0.

A general term in the perturbation series for $\bar{N}^{\text{open}}$ consists of a collection of boxes in which there may be an arbitrary number of $-Z$ vertices appearing either on the open valence lines or on the valence lines inside the boxes and on the lines joining the boxes. The effects of such $-Z$ insertions on the open lines and on those lines joining the boxes may be accounted for *exactly* by replacing the $\bar{N}^0$ corresponding to these lines by $\bar{N}_F^0$, as implied by Fig. 12. Thus, a typical member of Σ^{BW} (corresponding to a top part) having any number of $-Z$ insertions on the open lines may be represented as in Fig. 13. If we now consider all of the $-Z$ insertions on the valence lines inside the boxes, then their effect can be summed up to infinite orders through a shifted denominator.[14] Thus, for the parent box shown in Fig. 14(a), collection of *all* the terms in which the valence line γ has all possible $-Z$ insertions results in
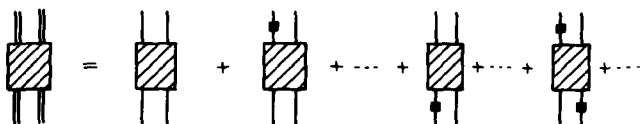

FIG. 13. It is shown how a collection of diagrams with a box and having any number of $-Z$ insertions on the open lines can be viewed as a box with renormalized open lines, such that the orbital energies for the open lines get shifted. The double lines in A2 correspond to such open lines. Therefore the unperturbed quantities $\bar{N}^0$ get modified to $\bar{N}_F^0$. This procedure thus serves to develop the open-shell perturbation theory where the model-space functions are not all degenerate.
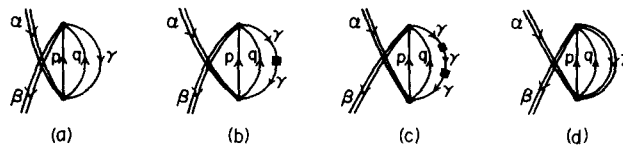

FIG. 14. Here we show how the series, starting with a "parent" box (a) and with one, two, $\ldots -Z$ insertions in the internal hole line γ [(b) and (c)], can be summed to all order leading to the shifted denominator expression (d) with a shifted orbital energy for γ [again shown by a double line in (d)].

a "shifted denominator expression" corresponding to Fig. 14(d) in which the "constant" orbital energy ϵ^v coming from γ gets replaced by the corresponding eigenvalue ϵ_γ^v with respect to f. The expression corresponding to Fig. 14(d), which is equivalent to all possible $-Z$ insertions on γ, as shown in Fig. 14(a)–14(c), is given by

$$-\frac{1}{2}\sum_{pq\gamma} \frac{\langle \beta\gamma | pq \rangle_a \langle pq | \alpha\gamma \rangle_a}{\omega + \epsilon^v - \epsilon_p - \epsilon_q}\left[1 + \sum_{n=1}^{\infty}\left(\frac{Z_\gamma^v}{\omega + \epsilon^v - \epsilon_p - \epsilon_q}\right)^n\right] \tag{A3}$$

$$= -\frac{1}{2}\sum_{pq\gamma} \frac{\langle \beta\gamma | pq \rangle_a \langle pq | \alpha\gamma \rangle_a}{\omega + (\epsilon^v - Z_\gamma^v) - \epsilon_p - \epsilon_q} = -\frac{1}{2}\sum_{pq\gamma} \frac{\langle \beta\gamma | pq \rangle_a \langle pq | \alpha\gamma \rangle_a}{\omega + \epsilon_\gamma^v - \epsilon_p - \epsilon_q} \ , \tag{A4}$$

where we have made use of Eq. (42).

The overall effect of these manipulations is the emergence of a perturbation theory in which the $\{\Phi_i\}$'s are nondegenerate with respect to an unperturbed Hamiltonian F, the associated unperturbed energies being $\bar{E}_0^i$, rather than the degenerate E_0^i, and the perturbation is $V' = H - F$.

In the subsequent discussion, we drop the double lines in favor of single lines, but remember that the partition of H can now be arbitrary.

It may now be said in hindsight that the Gellman–Low theorem, [Eq. (4)], can be postulated for an arbitrary partition of H into $H_0 + V$, even when the $\{\Phi_i\}$'s are not necessarily degenerate with respect to H_0.[12] We should mention here that a corresponding approach in the time-independent framework for treating nondegenerate $\{\Phi_i\}$ was also put forward by Brandow.[4]

APPENDIX B

In this appendix we discuss the details of the time integration procedure for calculating the contributions from the folded boxes both for the individual boxes and for the MC and TC corrections that arise when a string of boxes is replaced by a string of points. We explicitly demonstrate the integration procedure for TC and MC terms arising from a string of two boxes. We follow essentially the JB[9] prescription except that the internal hole and particle valence lines are treated *symmetrically* in our development.
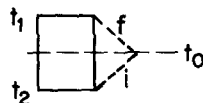

FIG. 15. A typical single-box folded diagram in which the incoming lines, labeled i, are below the outgoing lines, labeled f. We call this an A1 type box.
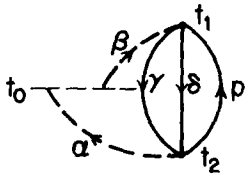
FIG. 16. A typical diagram, corresponding to the box structure of Fig. 15, which is symmetric around the folding time t_0. This gives a Hermitian contribution to $\Sigma_{\alpha\beta}$.

1. Contributions from single boxes

In this subsection, we consider single boxes in which *all* the external valence lines enter at one vertex and leave from another vertex. In subsection 4, we treat the other types of single-box situations.

Case 1: Figure 15 shows a typical single-box diagram, in which the labels f and i appear on the folded lines attached to the later and earlier times t_1 and t_2, respectively. We shall henceforth call this an A1 type box. The lines i or f may, in general, be a group of valence lines (holes and/or particles) contributing a factorlike $W = \Sigma_h \epsilon_h - \Sigma_p \epsilon_p$ for the respective time intervals (as discussed in Sec. VA). The time-dependent part which contributes to the denominators of such a folded box is

$$\frac{1}{D_{if}} = (-i) \int_0^\infty d(t_1 - t_2) \exp[iW_f(t_0 - t_1)]$$
$$\times \exp[iW_i(t_2 - t_0)] \exp[iW_1(t_1 - t_2)] . \tag{B1}$$

To perform the time integrations we write the time base t_0 as

$$t_0 = \rho_1 t_1 + \rho_2 t_2 , \tag{B2}$$

with

$$\rho_1 + \rho_2 = 1 . \tag{B3}$$

Here, ρ_1 and ρ_2 are to be adjusted to ensure Hermiticity of Σ. Writing $(t_0 - t_1)$ and $(t_2 - t_0)$ in terms of the integration variable $(t_1 - t_2)$, we obtain

$$t_0 - t_1 = (\rho_1 - 1)(t_1 - t_2) \tag{B4}$$

and

$$t_2 - t_0 = -\rho_1(t_1 - t_2) . \tag{B5}$$

FIG. 18. A typical single-box diagram where the incoming lines, labeled i, join the box above the outgoing lines, labeled f. We call this an A2 type box.

Hence, the denominator D_{if} is

$$D_{if} = [W_f(\rho_1 - 1) - W_i \rho_1 + W_1] . \tag{B6}$$

Choosing t_0 to lie midway between t_1 and t_2 $(\rho_1 = \rho_2 = \frac{1}{2})$, yields

$$D_{if} = [W_1 - \tfrac{1}{2}(W_i + W_f)] . \tag{B7}$$

The denominator D_{if} is thus always symmetric under the interchange of the labels i and f. The numerator N_{if} corresponding to such a box will only be symmetric under the interchange of labels i and f if the diagram corresponding to the box is symmetric about t_0, leading to an expression N_{if}/D_{if} for the diagram which is symmetric. For a diagram which is not symmetric about t_0, there always exists a conjugate diagram in Σ such that the two are related to each other via a reflection through a horizontal mirror plane at t_0 but preserving the sense of arrows of the diagram. The denominators of both these diagrams are the same for our choice of t_0. Denoting the numerators for these diagrams as N_{if} and N_{if}^r, one has

$$N_{if}^r = N_{fi} , \tag{B8}$$

giving a symmetric expression for the sum of these two diagrams as $(N_{if} + N_{fi})/D_{if}$. To illustrate these cases, let us consider some typical examples. Figure 16 shows a diagram which is symmetric around t_0. For this diagram we have

$$W_f = \epsilon_\beta, \quad W_i = \epsilon_\alpha, \quad W_1 = \epsilon_\gamma + \epsilon_\delta - \epsilon_p .$$

The overall contribution of the diagram, which is symmetric under interchange of α and β, is given by

$$\frac{1}{2} \sum_{\gamma\delta p} \frac{\langle \gamma\delta|\beta p\rangle_a \langle \alpha p|\gamma\delta\rangle_a}{[\epsilon_\gamma + \epsilon_\delta - \epsilon_p - \frac{1}{2}(\epsilon_\alpha + \epsilon_\beta)]} . \tag{B9}$$

Figures 17(a) and 17(b) show two diagrams, each of which is not symmetric about t_0, but which together give a symmetric contribution:

$$-\sum_{\substack{\mu\gamma\delta \\ pq}} \frac{(\langle\mu\delta|qp\rangle_a \langle\gamma q|\beta\mu\rangle_a \langle\alpha p|\gamma\delta\rangle_a + \langle\gamma\delta|\beta p\rangle_a \langle\alpha\mu|\gamma q\rangle_a \langle qp|\mu\delta\rangle_a)}{(\epsilon_\mu + \epsilon_\delta - \epsilon_q - \epsilon_p)[\epsilon_\gamma + \epsilon_\delta - \epsilon_p - \frac{1}{2}(\epsilon_\alpha + \epsilon_\beta)]} . \tag{B10}$$
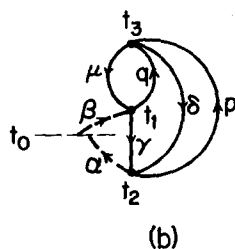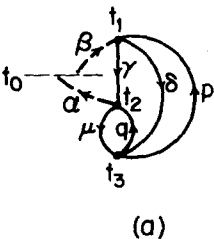

(a)

(b)

FIG. 17. (a) and (b) are two diagrams which are mirror images of each other. They correspond to the box structure of Fig. 15 and are not symmetric around t_0. The two together give a Hermitian contribution to $\Sigma_{\alpha\beta}$.
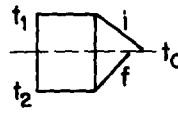
Figure 17 might be viewed as belonging to the box of the Fig. 15 in which there are additional time vertices appearing beyond the interval t_1, t_2. The integration variables for such cases, typified by Fig. 17(a), would be $(t_1 - t_2)$ and $(t_2 - t_3)$.

We emphasize here that our definition of "point" includes contributions from all internal lines of the box, be they particles or holes. This leads to a symmetric treatment of the internal hole and particle lines. In contrast, JB[9] perform the folding in such a way that the internal hole lines are treated as external to the box, leading to a point with bubbles. In our folding proce-
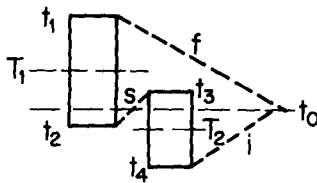
FIG. 19. A double box model-correcting diagram with an A1-A1 type combination for the boxes.

FIG. 20. A typical model-correcting diagram with the box structure of Fig. 19.

dure, *symmetric* treatment of internal hole and particle line is possible since the operators appearing in Σ [see Eq. (53)] are in normal order, which therefore already includes the effect of bubbles. Thus the *contributions* of a folded box in our scheme would be *different* from that of the JB scheme.

Case 2: Figure 18 shows a typical single-box diagram in which it was not necessary to fold the external valence lines. We call this an A2 type box. Here the time-dependent part contributing to the denominator is

$$\frac{1}{D_{if}} = (-i) \int_0^\infty d(t_1 - t_2) \exp[iW_f(t_0 - t_2)]$$

$$\times \exp[iW_i(t_1 - t_0)] \exp[iW_1(t_1 - t_2)] \ . \quad (B11)$$

Using $t_0 = \frac{1}{2}t_1 + \frac{1}{2}t_2$, one obtains a symmetric expression for D_{if}:

$$D_{if} = \tfrac{1}{2}(W_i + W_f) + W_1 \ . \quad (B12)$$

The symmetry of the corresponding numerator again depends upon the symmetry of the diagram around t_0,

and the considerations discussed for case 1 again apply here directly. From the above cases of single boxes one has six double-box correcting diagrams, three MC and three TC, which we discuss now.

2. Contributions from double-box model-correcting diagrams

Case 1: Figure 19 shows one typical MC diagram in which both the external valence lines are folded. This double-box diagram is an A1-A1 type combination. T_1 and T_2 correspond to the points of folding of individual boxes; the model-correcting situation arises in the time ranges $t_2 < t_3$ and $T_1 \geq T_2$, with $T_1 = \frac{1}{2}(t_1 + t_2)$ and $T_2 = \frac{1}{2}(t_3 + t_4)$. The integration variables that we choose to obtain the denominator are $(t_1 - t_2)$, $(t_3 - t_4)$, and $(t_3 - t_2)$. From the inequality between T_1 and T_2, we find

$$t_3 - t_2 \leq \tfrac{1}{2}(t_1 - t_2 + t_3 - t_4) \ .$$

Thus the time-dependent part contributing to the denominator is given by

$$\frac{1}{D_{if}} = (-i)^3 \int_0^\infty d(t_1 - t_2) \int_0^\infty d(t_3 - t_4) \int_0^{(1/2)(t_1-t_2)+(1/2)(t_3-t_4)} d(t_3 - t_2)$$

$$\times \exp[iW_1(t_1 - t_2)] \exp[iW_3(t_3 - t_4)] \exp[iW_f(t_0 - t_1)] \exp[iW_i(t_4 - t_0)] \exp[iW_s(t_3 - t_2)] \ , \quad (B13)$$

where W_1, for example, is the W factor within the time interval $(t_1 - t_2)$. Let us note that the factor W_s for the internal folded line labeled s appears with a negative sign.

Choosing t_0 as

$$t_0 = \rho_1 t_1 + \rho_2 t_2 + \rho_3 t_3 + \rho_4 t_4 \ , \quad (B14)$$

with $\sum_i \rho_i = 1$, we have

$$t_0 - t_1 = (\rho_1 - 1)(t_1 - t_2) + (\rho_1 + \rho_2 + \rho_3 - 1)(t_3 - t_4) + (1 - \rho_1 - \rho_2)(t_3 - t_2) \ , \quad (B15)$$

$$t_4 - t_0 = -\rho_1(t_1 - t_2) - (\rho_1 + \rho_2 + \rho_3)(t_3 - t_4) + (\rho_1 + \rho_2)(t_3 - t_2) \ . \quad (B16)$$
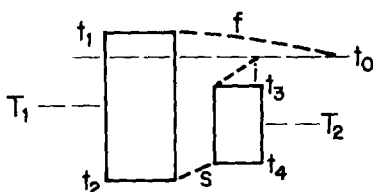
The expression (B5) then yields

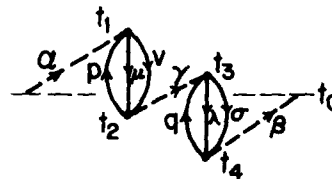FIG. 21. A double-box model-correcting diagram with an A1-A2 combination for the boxes.

FIG. 22. A double-box model-correcting diagram with an A2-A1 combination for the boxes.
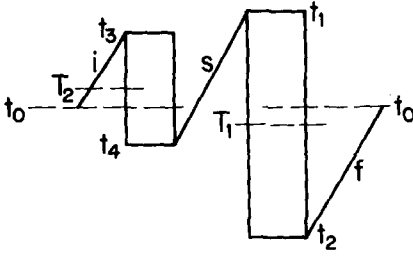
FIG. 23. A double-box true-correcting diagram with an A2–A2 combination for the boxes.
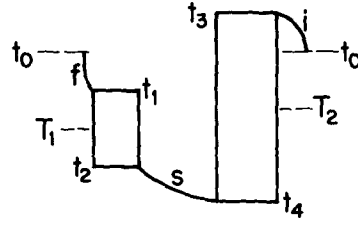

FIG. 24. A double-box true-correcting diagram with an A1–A2 type combination for the boxes.

$$1/D_{if} = 1/\{[W_1 + (\rho_1 - 1)W_f - \rho_1 W_i][W_2 - \rho_4 W_f - (1 - \rho_4)W_i]$$

$$\times [(1 - \rho_1 - \rho_2)W_f + (\rho_1 + \rho_2)W_i - W_s]\} - 1/\{[W_1 + \tfrac{1}{2}(\rho_1 - \rho_2 - 1)W_f + \tfrac{1}{2}(\rho_2 - \rho_1)W_i - \tfrac{1}{2}W_s]$$

$$\times [W_3 + (\tfrac{1}{2}\rho_1 + \tfrac{1}{2}\rho_2 + \rho_3 - \tfrac{1}{2})W_f - (\tfrac{1}{2}\rho_1 + \tfrac{1}{2}\rho_2 + \rho_3)W_i - \tfrac{1}{2}W_s][(1 - \rho_1 - \rho_2)W_f + (\rho_1 + \rho_2)W_i - W_s]\} \; . \tag{B17}$$

To make this denominator symmetric in the i and f labels one has to take

$$\rho_1 = \tfrac{1}{2}, \quad \rho_2 = 0, \quad \rho_3 = 0, \quad \rho_4 = \tfrac{1}{2} \; ,$$

which means that t_0 is midway between t_1 and t_4. We then have

$$1/D_{if} = 1/\{[W_1 - \tfrac{1}{2}(W_i + W_f)][W_3 - \tfrac{1}{2}(W_i + W_f)][\tfrac{1}{2}(W_f + W_i) - W_s]\}$$

$$- 1/\{[W_1 - \tfrac{1}{2}W_s - \tfrac{1}{4}(W_f + W_i)][W_3 - \tfrac{1}{2}W_s - \tfrac{1}{4}(W_f + W_i)][\tfrac{1}{2}(W_f + W_i) - W_s]\} \; . \tag{B18}$$

The symmetry of the numerator, as discussed earlier, again depends upon the symmetry of the diagram around t_0. For the specific fourth-order diagram shown in Fig. 20, one has

$$W_f = \epsilon_\alpha, \quad W_i = \epsilon_\beta, \quad W_1 = \epsilon_\mu + \epsilon_\nu - \epsilon_p, \quad W_3 = \epsilon_\lambda + \epsilon_\sigma - \epsilon_q, \quad W_s = \epsilon_\gamma \; .$$

The contribution of this diagram to Σ is

$$\frac{1}{4} \sum_{\mu\nu\lambda\sigma\gamma,pq} \frac{\langle \mu\nu | \alpha p \rangle_a \langle \lambda\sigma | \gamma q \rangle_a \langle \gamma p | \mu\nu \rangle_a \langle \beta q | \lambda\sigma \rangle_a}{D_{\alpha\beta}} \; , \tag{B19}$$

where

$$1/D_{\alpha\beta} = 1/\{[\epsilon_\mu + \epsilon_\nu - \epsilon_p - \tfrac{1}{2}(\epsilon_\alpha + \epsilon_\beta)][\epsilon_\lambda + \epsilon_\sigma - \epsilon_q - \tfrac{1}{2}(\epsilon_\alpha + \epsilon_\beta) - \epsilon_\gamma]\}$$

$$- 1/\{[\epsilon_\mu + \epsilon_\nu - \epsilon_p - \tfrac{1}{2}\epsilon_\gamma - \tfrac{1}{4}(\epsilon_\alpha + \epsilon_\beta)][\epsilon_\lambda + \epsilon_\sigma - \epsilon_q - \tfrac{1}{2}\epsilon_\gamma - \tfrac{1}{4}(\epsilon_\alpha + \epsilon_\beta)][\tfrac{1}{2}(\epsilon_\alpha + \epsilon_\beta) - \epsilon_\gamma]\} \; . \tag{B20}$$

Case 2: Figure 21 shows another type of MC diagram involving an A1–A2 combination. The MC situation arises in the time range $T_1 = \tfrac{1}{2}(t_1 + t_2) \geq T_2 = \tfrac{1}{2}(t_3 + t_4)$ with $t_2 < t_4$. The pertinent integration variables are $(t_1 - t_3)$, $(t_3 - t_4)$, and $(t_4 - t_2)$, of which only $(t_4 - t_2)$ goes over finite limits $0 \leq t_4 - t_2 \leq t_1 - t_3$. Thus we have

$$1/D_{if} = (-i)^3 \int_0^\infty d(t_1 - t_3) \int_0^\infty d(t_3 - t_4) \int_0^{t_1 - t_3} d(t_4 - t_2) \exp[iW_1(t_1 - t_2)] \exp[iW_3(t_3 - t_4)] \exp[-iW_s(t_4 - t_2)] \; . \tag{B21}$$

Proceeding as before with $t_0 = \rho_1 t_1 + \rho_2 t_2 + \rho_3 t_3 + \rho_4 t_4$, and choosing the ρ_i's to ensure symmetry of D_{if}, we obtain $\rho_1 = \tfrac{1}{2}$, $\rho_2 = \rho_4 = 0$, $\rho_3 = \tfrac{1}{2}$, and

$$1/D_{if} = 1/\{[2W_1 - W_s - \tfrac{1}{2}(W_i + W_f)][W_1 - \tfrac{1}{2}(W_i + W_f)][W_1 + W_3]\} \; . \tag{B22}$$

Case 3: Figure 22 shows an MC diagram involving an A2–A1 combination, which is the mirror image of Fig. 21. The contribution to the corresponding denominator may be obtained by interchanging W_1 and W_3 in Eq. (B22).

3. Contributions from double-box true-correcting diagrams

Case 1: Figure 23 shows a true-correcting diagram of the type A2–A2. The true-correcting diagram arises in the time range $t_1 > t_4$ and $T_2 > T_1$ with $T_1 = \tfrac{1}{2}(t_1 + t_2)$, $T_2 = \tfrac{1}{2}(t_3 + t_4)$. The time variables for the integration are $(t_1 - t_2)$, $(t_3 - t_4)$, and $(t_1 - t_4)$. The contribution to the denominator is given by

$$1/D_{if} = (-i)^3 \int_0^\infty d(t_1 - t_2) \int_0^\infty d(t_3 - t_4) \int_0^{(1/2)(t_1 - t_2) + (t_3 - t_4)} d(t_1 - t_4)$$

$$\times \exp[iW_1(t_1 - t_2)] \exp[iW_2(t_3 - t_4)] \exp[iW_s(t_1 - t_4)] \exp[iW_f(t_0 - t_2)] \exp[iW_i(t_3 - t_0)] \; . \tag{B23}$$

Defining $t_0 = \rho_1 t_1 + \rho_2 t_2 + \rho_3 t_3 + \rho_4 t_4$, and choosing the ρ_i's as $\rho_1 = \rho_4 = 0$, $\rho_2 = \rho_3 = \tfrac{1}{2}$, gives the symmetric denominator
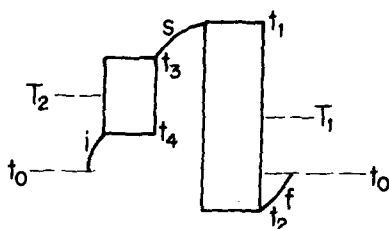
FIG. 25. A double-box true-correcting diagram with A2-A1 type combination for the boxes.

$$1/D_{if} = 1/\{[W_1 + \tfrac{1}{2}(W_i + W_f)][W_3 + \tfrac{1}{2}(W_i + W_f)]$$
$$\times [W_s - \tfrac{1}{2}(W_i + W_f)]\} - 1/\{[W_1 + \tfrac{1}{2}W_s + \tfrac{1}{4}(W_i + W_f)]$$
$$\times [W_3 + \tfrac{1}{2}W_s + \tfrac{1}{4}(W_i + W_f)][W_s - \tfrac{1}{2}(W_i + W_f)]\} . \quad (B24)$$

Case 2: Figure 24 shows a true-correcting diagram of the type A1-A2. The true-correcting situation arises in the range $T_1 = \tfrac{1}{2}(t_1 + t_2) < T_2 = \tfrac{1}{2}(t_3 + t_4)$, with $t_2 > t_4$. The variables are $(t_1 - t_2)$, $(t_2 - t_4)$, and $(t_3 - t_1)$. The contribution to the denominator is

$$1/D_{if} = (-i)^3 \int_0^\infty d(t_3 - t_1) \int_0^\infty d(t_1 - t_2) \int_0^{t_3 - t_1} d(t_2 - t_4)$$
$$\times \exp[iW_1(t_1 - t_2)] \exp[iW_3(t_3 - t_4)] \exp[iW_s(t_2 - t_4)]$$
$$\times \exp[iW_f(t_0 - t_1)] \exp[iW_i(t_3 - t_0)] . \quad (B25)$$

Introducing $t_0 = \rho_1 t_1 + \rho_2 t_2 + \rho_3 t_3 + \rho_4 t_4$, and choosing $\rho_1 = \rho_3 = \tfrac{1}{2}$, $\rho_2 = \rho_4 = 0$ to ensure symmetry of D_{if}, we have

$$1/D_{if} = 1/\{[W_3 + \tfrac{1}{2}(W_i + W_f)]$$
$$\times [2W_3 + \tfrac{1}{2}(W_i + W_f) + W_s][W_1 + W_3]\} . \quad (B26)$$

Case 3: Figure 25 shows a true-correcting diagram of the type A2-A1, which is the mirror-image of Fig. 24. The contribution to its D_{if} is obtained by interchanging W_1 and W_3 in Eq. (B26).

4. Single-box diagrams with multiple energy and exit points

Such types of diagrams are too numerous to be given an exhaustive treatment here. However, the expressions for their denominators follow a general pattern and it suffices to discuss here a typical example in Fig. 26. Here, for $t_0 = \tfrac{1}{2}(t_1 + t_2)$ the symmetric denominator is

$$D_{p\alpha,q\beta} = \tfrac{1}{2}(\epsilon_\alpha + \epsilon_\beta + \epsilon_p + \epsilon_q) - \epsilon_r - \epsilon_s .$$

5. Summary of the diagram rules

Except for the single-box diagrams discussed in subsections 1 and 4, there are no easily stated general rules for calculating the denominators. For the multiple boxes from which TC and MC terms arise, one needs to follow the time integration procedure as discussed in subsections 2 and 3. However, there are general rules for the numerator of any diagram. Following are the general rules for evaluating the numerator for the general case and the denominator of the single-box case: for the numerator, (a) apply the conventional Goldstone-Hugenholz rules and (b) attach an additional sign factor (−1) for each pair of vertices joined by folded internal
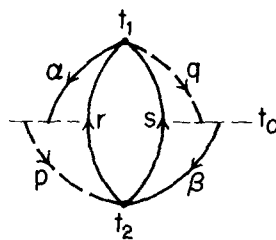

FIG. 26. A representative single-box type diagram in which there are more than one entry and exit points. In this example, a hole-particle pair (α, p) are ingoing lines and another hole-particle pair (β, q) are outgoing lines. However, α enters at time t_1, while p enters at a different time t_2. Similarly, β comes out at time t_2, while q comes out at t_1.

valence lines; for the denominator of single boxes, for each pair of successive vertices of a folded box, attach a factor $\Sigma_h \epsilon_h - \Sigma_p \epsilon_p + \tfrac{1}{2}(\Sigma_d \epsilon_d - \Sigma_u \epsilon_u)$. Here h and p are the internal hole and particle lines between these two vertices, respectively; d and u are the downgoing and upgoing external lines, respectively, including the folded external lines.

[1] A. Banerjee, D. Mukherjee, and J. Simons, J. Chem. Phys. **76**, 1972 (1982).

[2] A. L. Fetter and J. D. Walecka, *Quantum Theory of Many-Particle Systems* (McGraw-Hill, New York, 1971).

[3] C. Bloch and J. Horowitz, Nucl. Phys. **8**, 91 (1958).

[4] B. Brandow, Rev. Mod. Phys. **39**, 771 (1967).

[5] V. Kvasnička, Czech J. Phys. B **24**, 605 (1974).

[6] I. Lindgren, J. Phys. B **7**, 2441 (1974).

[7] T. T. S. Kuo, S. Y. Lee, and K. Ratcliffe, Nucl. Phys. A **176**, 65 (1971).

[8] G. Oberlechner, F. Owono-N-Gruema, and J. Richert, Nuovo Cimento B **68**, 23 (1970).

[9] M. B. Johnson and M. Baranger, Ann. Phys. (N.Y.) **62**, 172 (1971).

[10] B. Brandow, in *Effective Interactions and Operators in Nuclei*, edited by B. R. Barett (Springer, Berlin, 1975).

[11] G. Hose and U. Kaldor, Phys. Scr. **2**, 357 (1980); G. D. Purvis and Y. Ohrn,

[12] See, e.g., K. F. Ratcliffe, in *Effective Interactions and Operators in Nuclei*, edited by B. R. Barett (Springer, Berlin, 1975).

[13] This follows in a straightforward fashion if we remember that there are appropriate step functions $\theta(t - t_1)$, etc., arising out of the T products.

[14] H. P. Kelly, Adv. Theor. Phys. **2**, 75 (1968).

[15] K. A. Bruckner, Phys. Rev. **100**, 36 (1955); J. Goldstone, Proc. R. Soc. London Ser. A **239**, 267 (1957).

[16] A. Messiah, *Quantum Mechanics* (Wiley, New York, 1962), Vol. 2.

[17] N. M. Hugenholtz, Physica (The Hague) **23**, 481 (1957).

[18] See, e.g., P. O. Löwdin, in *Perturbation Theory and its Applications in Quantum Mechanics*, edited by C. H. Wilcox (Wiley, New York, 1966).

[19] A. Mukhopadhyay, R. K. Moitra, and D. Mukherjee, Int. J. Quantum Chem. **9**, 545 (1975).

[20] P. Westhaus, E. G. Bradford, and D. Hall, J. Chem. Phys. **62**, 1607 (1975); D. Mukherjee, R. K. Moitra, and A. Mukhopadhyay, Pramana **9**, 545 (1977); I. Shavitt and L. T. Redmon, J. Chem. Phys. **73**, 5711 (1980).

[21] B. H. Brandow, Int. J. Quantum Chem. **15**, 207 (1979); D. J. Klein, J. Chem. Phys. **61**, 786 (1974); F. Jorgensen, Mol. Phys. **29**, 1137 (1975).